(1) PRILIMINARY STUDY ON SUPER-FERRIC MAGNET WITH SELF-CORRECTION COILS

(2) WIRE MOTION SYSTEM

SOKENDAI STUDENT (October 2006)
Department of Accelerator Science
Crab Cavity Group
Kailash RUWALI
kailash_ruwali@yahoo.com

OUTLINE

- Principle
- Motivation
- Strategy
- Features
- Mechanism of Self-Correction Coil (SCC)
- Design Philosophy
- Fabrication Aspects
- Measurement Scheme

Principle

- The Self-Correction Coils (SCC) are shorted superconducting correction coil set inside the magnet aperture.

- SCC scheme will cancel the error field (produced irrespective of their origin) automatically within the magnet aperture.

- The operation principle of the SCC is based on an inductive phenomenon.

- The error field present inside the magnet aperture will induce current in the SCC. The induced current thus cancels the error field.

Motivation

- Approach to get compact relatively high magnetic field. Useful for SRS in the range of few GeV, compact accelerators for Commercial applications like Lithography and also in Medical applications like Angiography.

- Low operation cost and its higher magnetic field than that of normal-conducting magnets.

- The use Super-Ferric Magnet (SFM) Technology will allow more choice in producing the field integral, and, hence, gives the optics designer more flexibility in choosing the most economical lattice.

- This kind of SFM with SCC has not yet developed.

Strategy

- ✓ Design and magnetic measurement of Super-Ferric magnet with self-correction coils to check

(1) effectiveness of the self-correcting coils

(2) dynamic range of the magnet system

Features

- Large dynamic range.
- Proposed Super-Ferric Magnet will operate at field level 2-3 T .
- Non-circular cross-section and curved SCC to incorporate the sagitta problem.
- Magnet system is compact, thus the overall size of the machine and total capital cost and operation cost reduces.

Contd…

- The major contribution to the magnetic field comes mostly from iron poles, rather than from windings. Thus, amount of superconductor needed reduces.

- Chances of magnet getting quench is rare since Lorentz force acting on coil is less, major flux goes through core.

- No active field correction (no additional winding into the air gap, the `Crenelation` technique, field correction by `holes in the poles` etc).

- Cost-driver analysis of VLHC → Superferric magnet is 2-3 times less costly per Tesla-meter than conventional superconducting magnets. (Source: Chap02_final_010106.doc, Stage -1 VLHC report)

Mechanism of Self-Correction Coil (SCC)

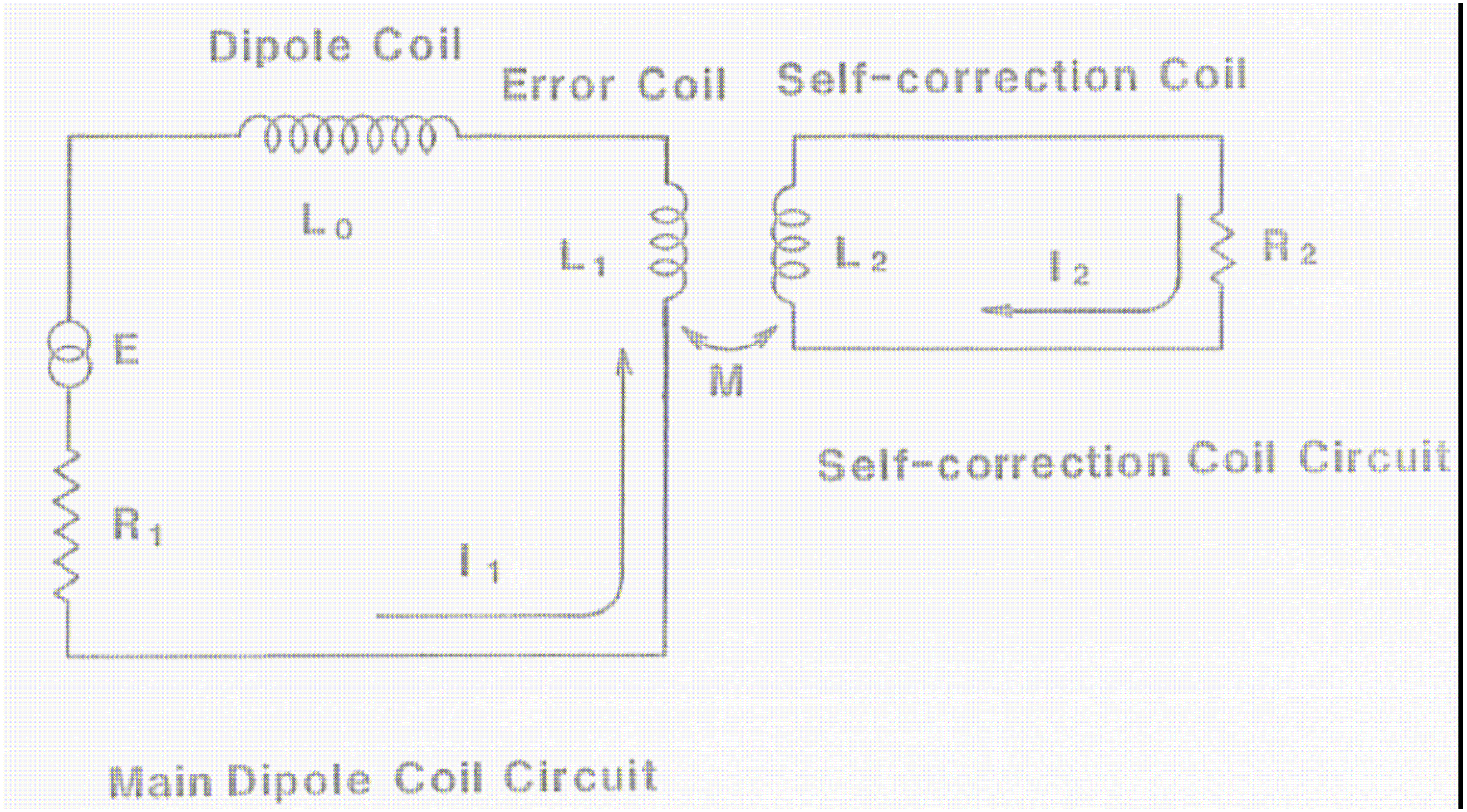

Model for ideal self-correction coil

- The currents, are determined by solving the following differential equations:

$$E = (L_o + L_1)\frac{dI_1}{dt} + I_1 R_1 + M\frac{dI_2}{dt}$$

$$0 = L_2\frac{dI_2}{dt} + I_2 R_2 + M\frac{dI_1}{dt}$$

$$L_2\frac{dI_2}{dt} = -M\frac{dI_1}{dt}$$

assuming $I_1=I_2=0$ at $t=0$,

$$I_2 = -M\frac{I_1}{L_2}$$

Contd…

- The strength of magnetic flux density B_1 produced by the error coil is:

$$B_1 = -\frac{\mu_0 n N_1 I_1}{2R_1}\left(\frac{r}{R_1}\right)^{n-1}\left\{1+\left(\frac{R_1}{b}\right)^{2n}\right\}$$

- The strength of magnetic flux density produced by the self-correction is:

$$B_2 = \frac{\mu_0 n N_1 I_1}{2R_1}\left(\frac{r}{R_1}\right)^{n-1}\left\{1+\left(\frac{R_1}{b}\right)^{2n}\right\} = -B_1$$

- In practical case, because error field induces many multipole components, to correct these error field components we need the same number of self-correction coil. Due to orthogonal property of each self-correction coil, there is no coupling between each self-correction coil.

NON-IDEAL, SINGLE BLOCK

SELF-CORRECTION COIL

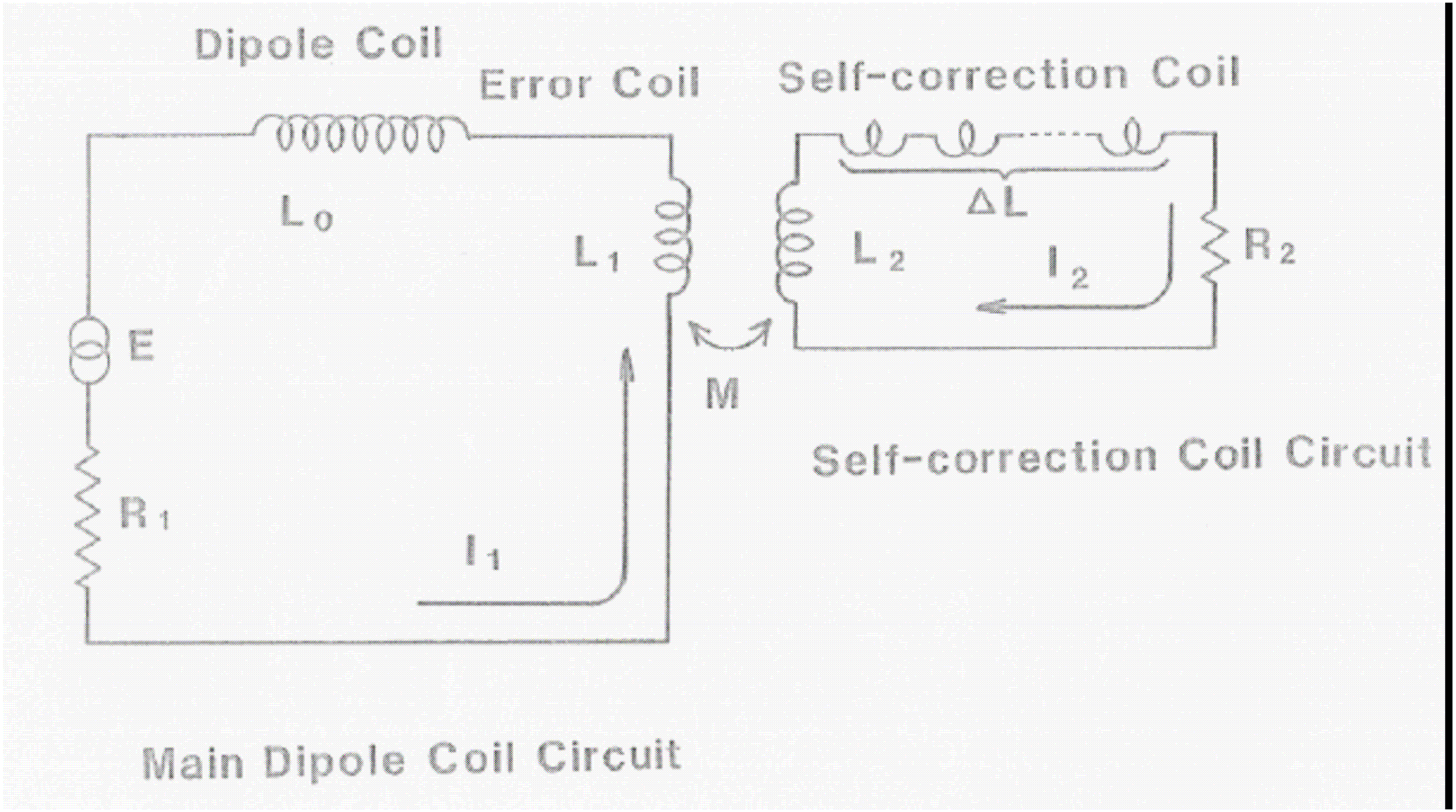

- The currents, are determined by solving the following differential equations:

$$E = (L_o + L_1)\frac{dI_1}{dt} + I_1 R_1 + M\frac{dI_2}{dt}$$

$$0 = (L_2 + \Delta L)\frac{dI_2}{dt} + I_2 R_2 + M\frac{dI_1}{dt}$$

$$(L_2 + \Delta L)\frac{dI_2}{dt} = -M\frac{dI_1}{dt}$$

assuming $I_1 = I_2 = 0$ at $t = 0$,

$$I_2 = -M\frac{I_1}{(L_2 + \Delta L)}$$

Contd…

- Introducing efficiency of self-correction coils as the ratio of induced magnetic field by the self-correction coil and error field as

$$\eta = \frac{B_2}{B_1}$$

- For single block approximation, efficiency is expressed as

$$\eta = \frac{\dfrac{\cos^2\theta_0 \sin^2\left(\dfrac{\delta\theta}{2}\right)}{\left(\dfrac{\delta\theta}{2}\right)^2}.\left\{1+\left(\dfrac{R_2}{b}\right)^{2n}\right\}}{\displaystyle\sum_{l=1}^{\infty}\dfrac{\cos^2\{(2l-1)\theta_0\}.\sin^2\left\{(2l-1).\dfrac{\delta\theta}{2}\right\}}{(2l-1)^3.\left(\dfrac{\delta\theta}{2}\right)^2}.\left\{1+\left(\dfrac{R_2}{b}\right)^{2n(2l-1)}\right\}}$$

- For single block, efficiency is less than unity, because of additional higher order mode contribution to self-inductance whereas for mutual inductance, contribution comes from fundamental mode only.

Design Philosophy

Main parameters of Superferric Dipole Magnet

Magnetic field in gap (T)	0.8
Aperture Gap (mm)	60
Total number of ampere-turns	30,000
Maximum current (A)	153
No. of turns	196
Dimension of magnet Length (mm) Width (mm) Height (mm)	 248 165 134

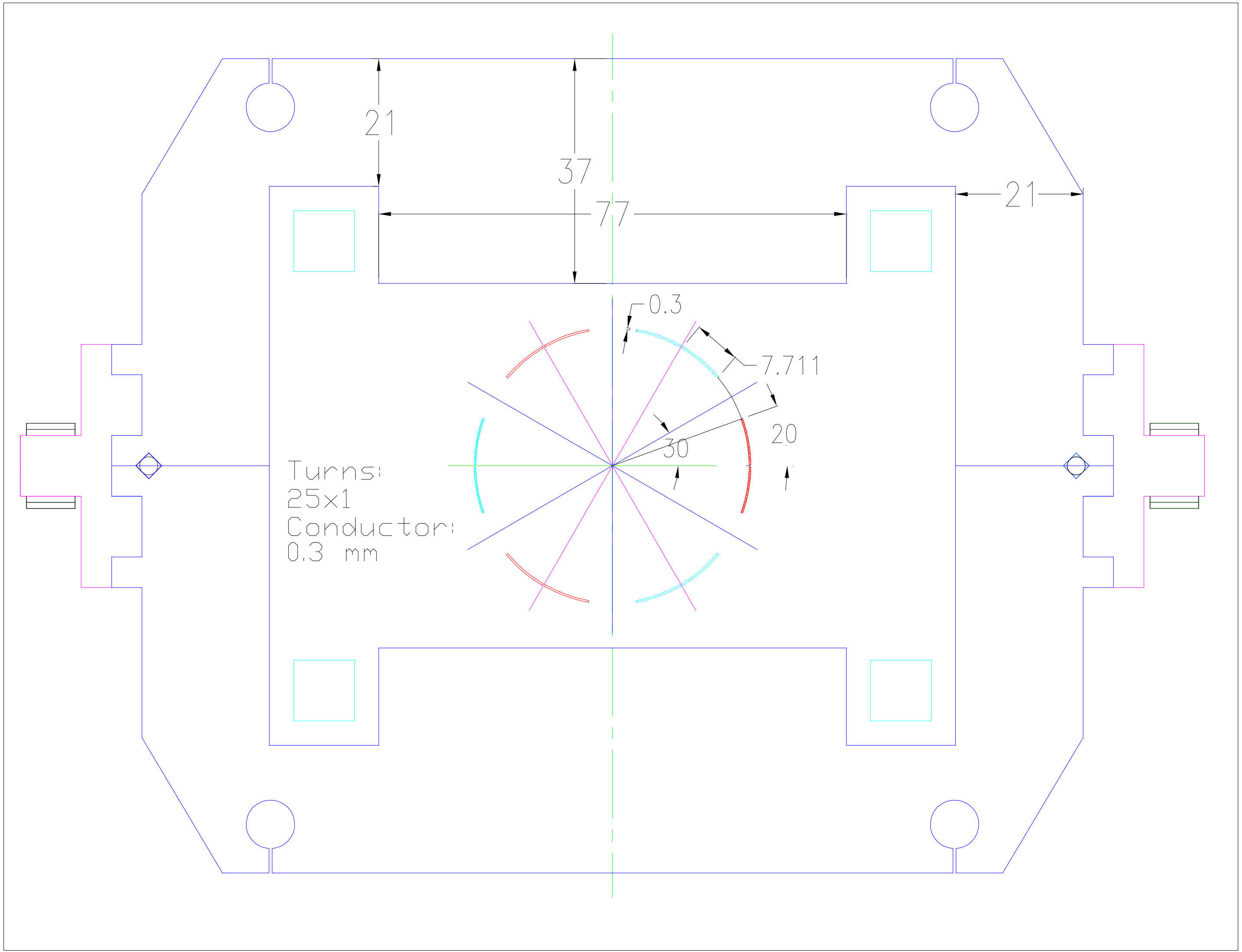

Sc wire characteristics

	Main Coil	Self-Correction Coil
Wire Diameter	0.7 mm	0.3 mm
Filament diameter	6 µm	0.1 µm
NbTi/Cu	1:1.8	1:3.45
Ic	383 A @ 4T 100 A @ 8.57 T	75 A @ 1T 32 A @ 2 T
Pitch length	30 mm	2 mm

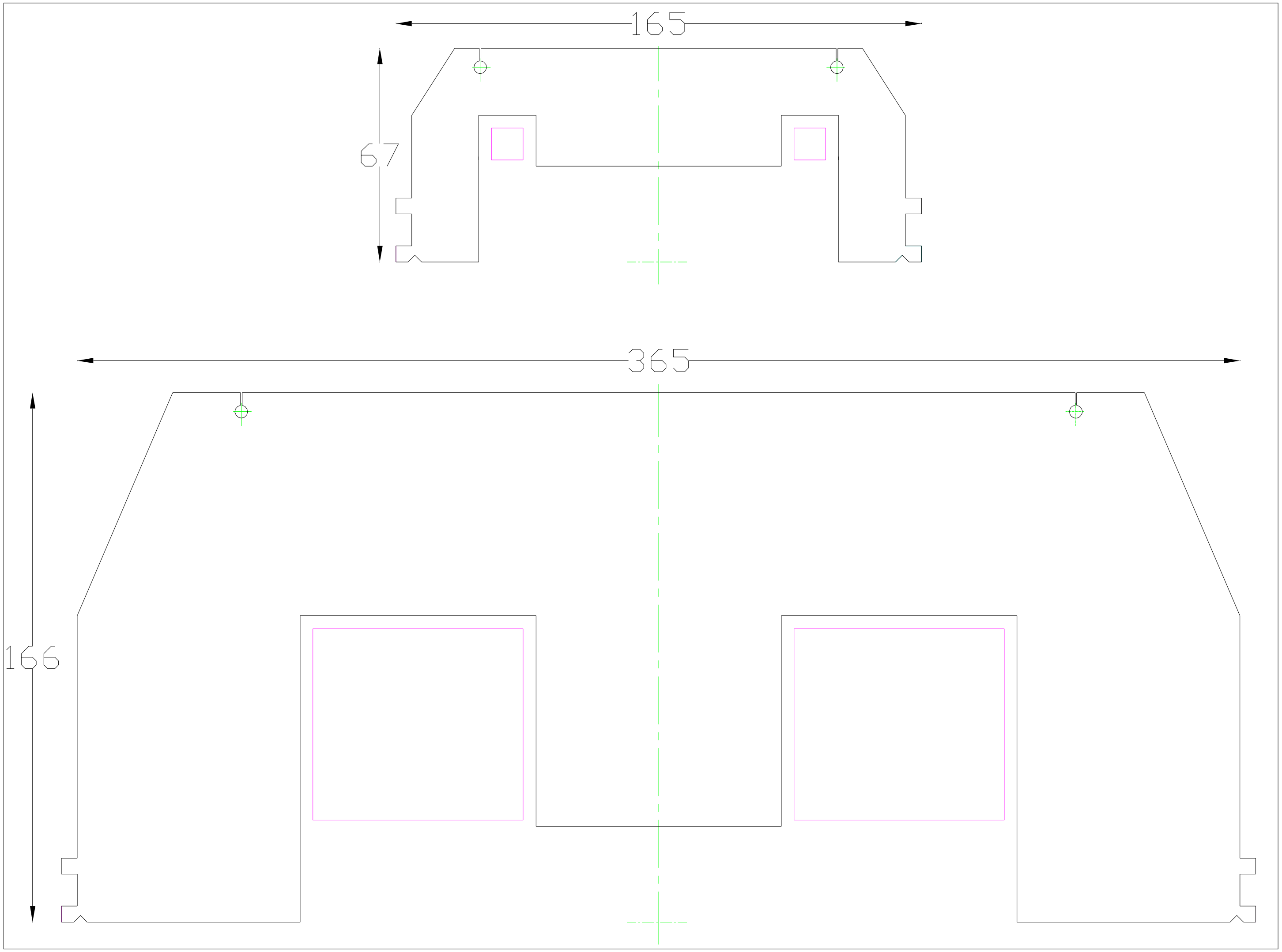

Turns (HxV)

(14x14)

J = 520 A/mm^2

P/S Rating

160 A, 6 V

Turns (HxV)

(11x10)

J = 10 A/mm^2

P/S Rating

180 A, 32 V

Superferric Magnet and Electromagnet Core comparison

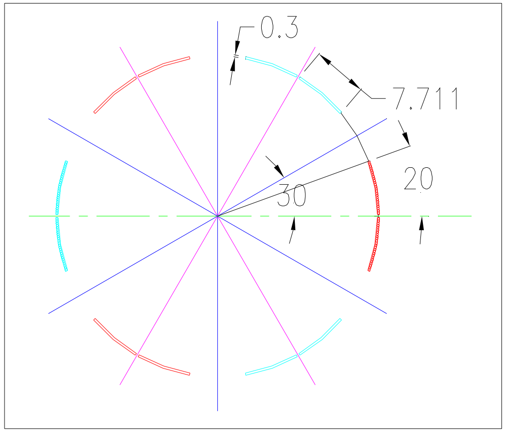

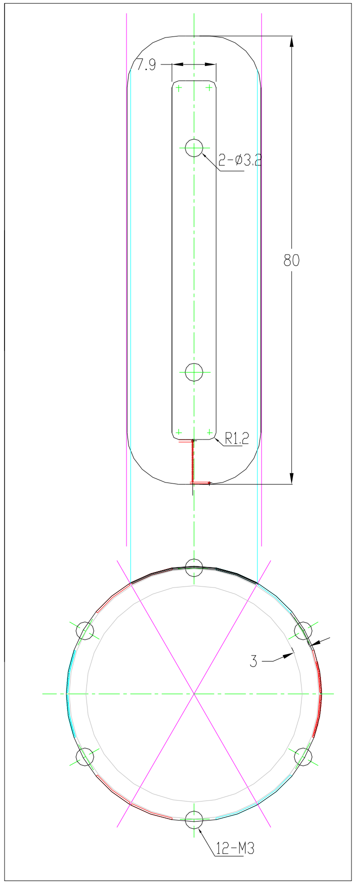

Turns	25X1
Conductor	
Diameter	0.3 mm
Coil ID	45 mm
Coil OD	45.3 mm

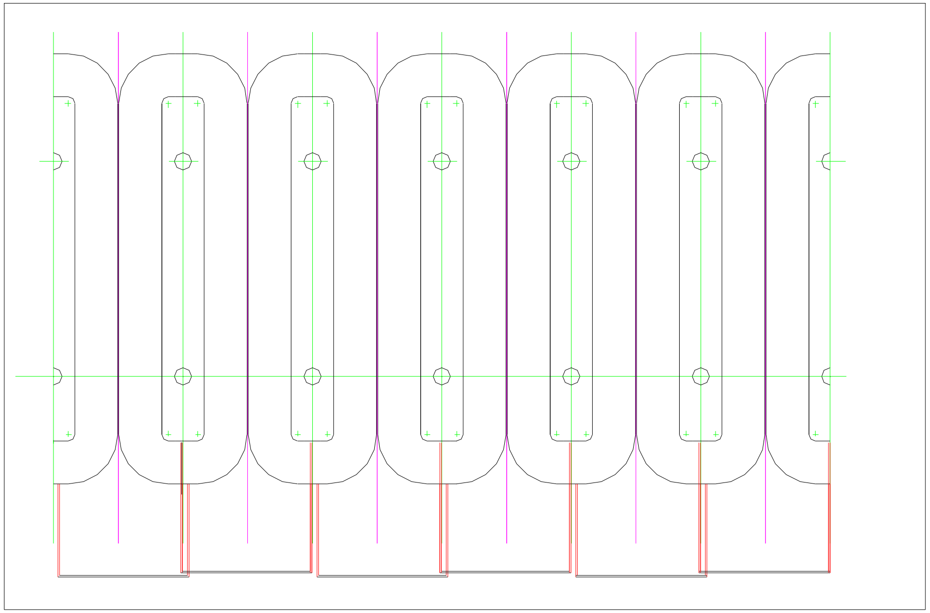

Shorted Self-correction Coil

Bussing Topology

Cross-section of Self-Correction Coil

No. of turns	196
Coil stacking	14x14
Wire Diameter (mm)	0.7
Coil size (mm)	9.8x9.8

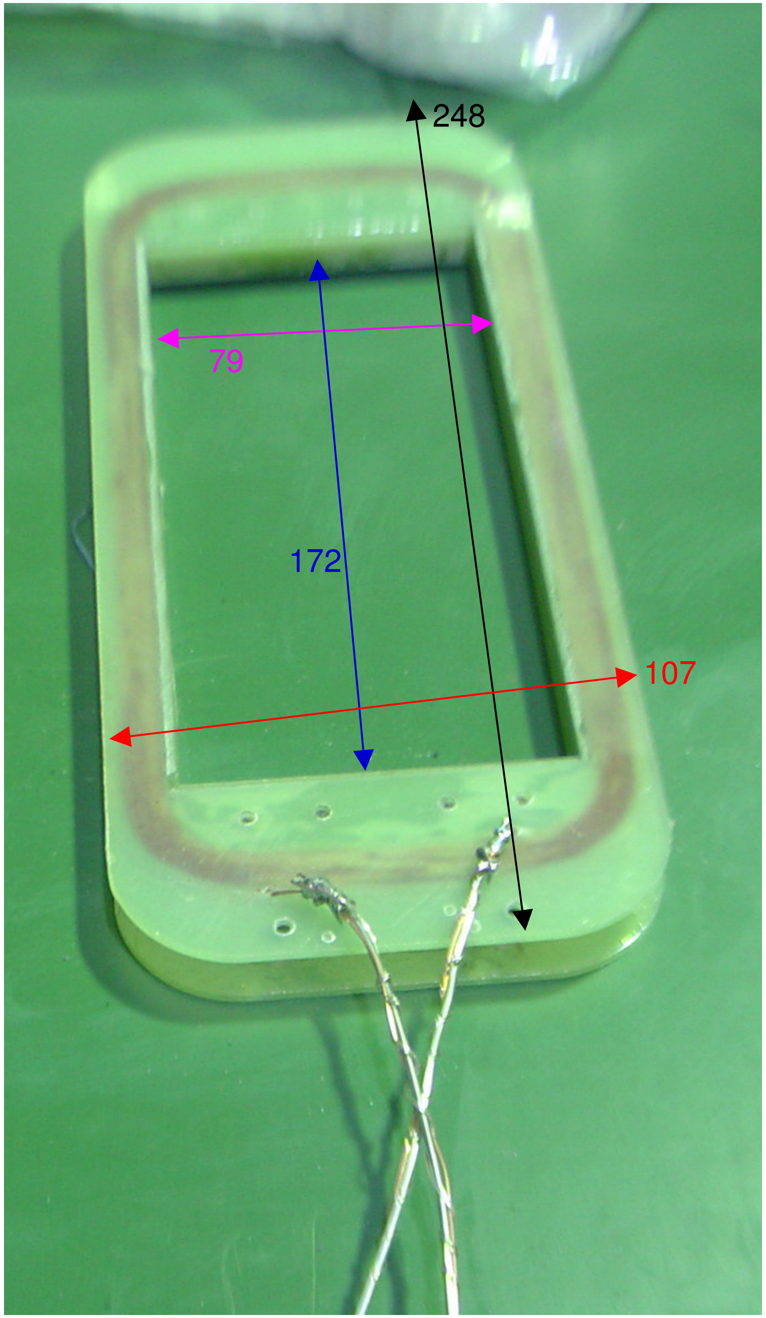


27 12 2007

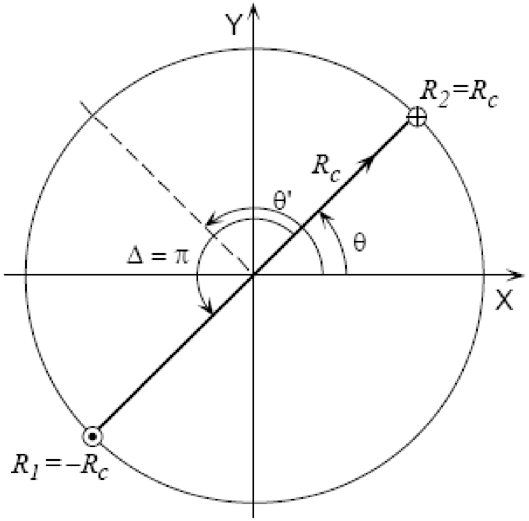

Cross-section of Dipole Coil

Parameters of rotating coil (Dipole coil)

Parameters	Values
No. of turns	80
Coil radius (mm)	15
Coil length (mm)	40

A dipole coil has a flat loop of wire arranged in such a way that the rotation axis passes through the center of the loop.

The flux through the coil

$$\phi_{Dipole}(\theta) = \sum_{\substack{n=1 \\ n=odd}}^{\infty} \frac{2NLR_{ref}}{n} \left(\frac{R_c}{R_{ref}} \right)^n C(n)\cos(n\theta - n\alpha_n)$$

It should be noted that the terms for even multipoles vanish in this particular geometry. A dipole coil is therefore sensitive to only the odd harmonics, i.e., dipole, sextupole, decapole, etc.

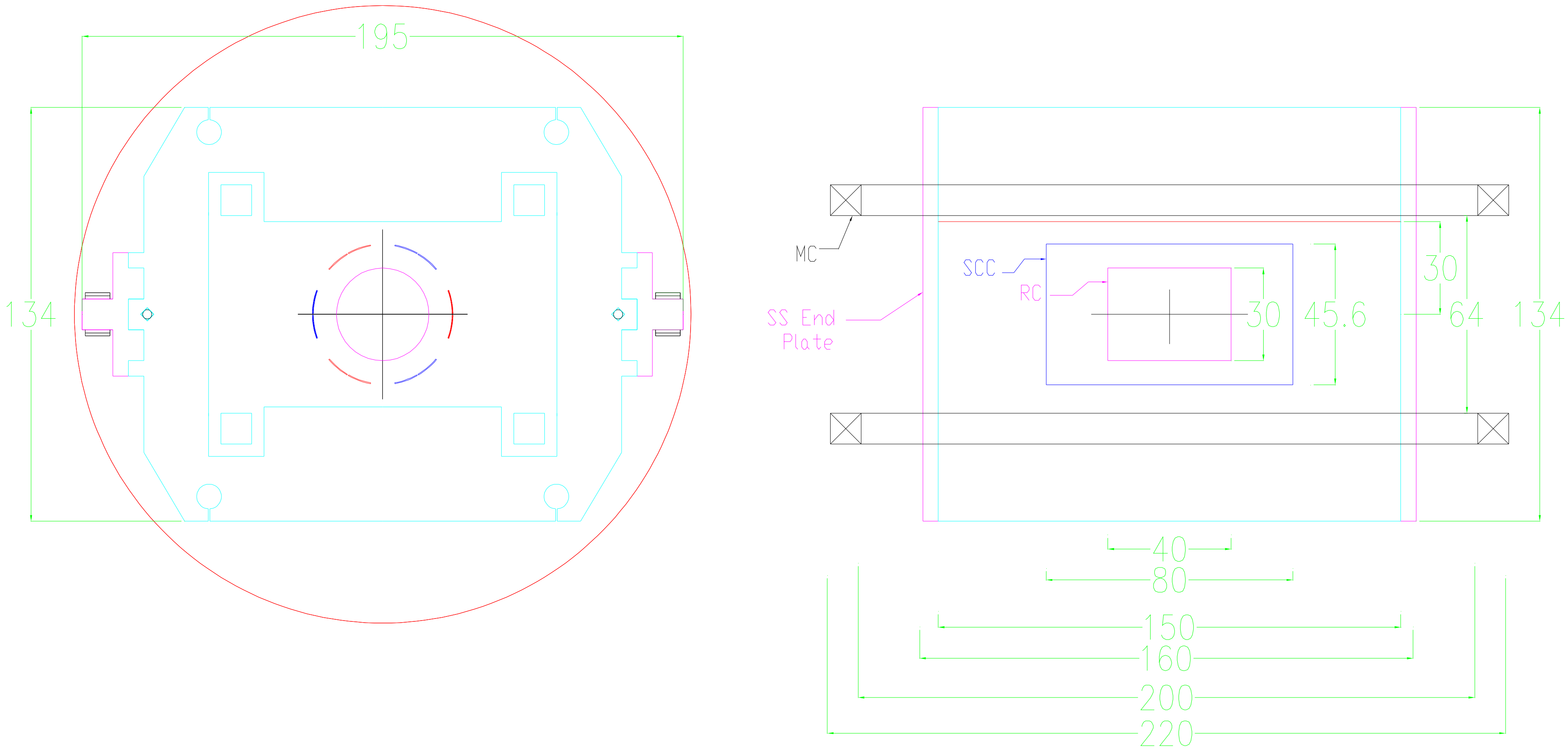

Plan view of Superferric magnet system

Wire Motion System

- Frictional heat is generated due to wire motion under various forces present in the winding: winding pretension, thermal and Lorentz forces.

- It can be generated wherever relative motion of conductor exist.

- The frictional losses depend on the thermal expansion and contraction properties of the bobbins and the winding tensions of the coil.

- The voltage generated in the coil is accompanied by two electromagnetic effects:

(i) an induced emf along the moved wire,

(ii) change of flux caused by the minute dislocation of current.

An experimental setup is designed to measure an induced emf generated by wire movement in the magnetic field.

Dynamic behavior of wire in magnetic force

- Wire movement can be pick up by measuring the voltage of sample.
- We can detect wire movement by observing spikes of the voltage.
- From the time profile of voltage we can estimate;

The displacement of wire and its speed.

1) Wire motion vs Cycle — Training effect
2) Wire motion vs Back up field **B**

   Reverse the back up field
3) Wire motion vs Tension **f**
4) Wire motion vs Insulation material

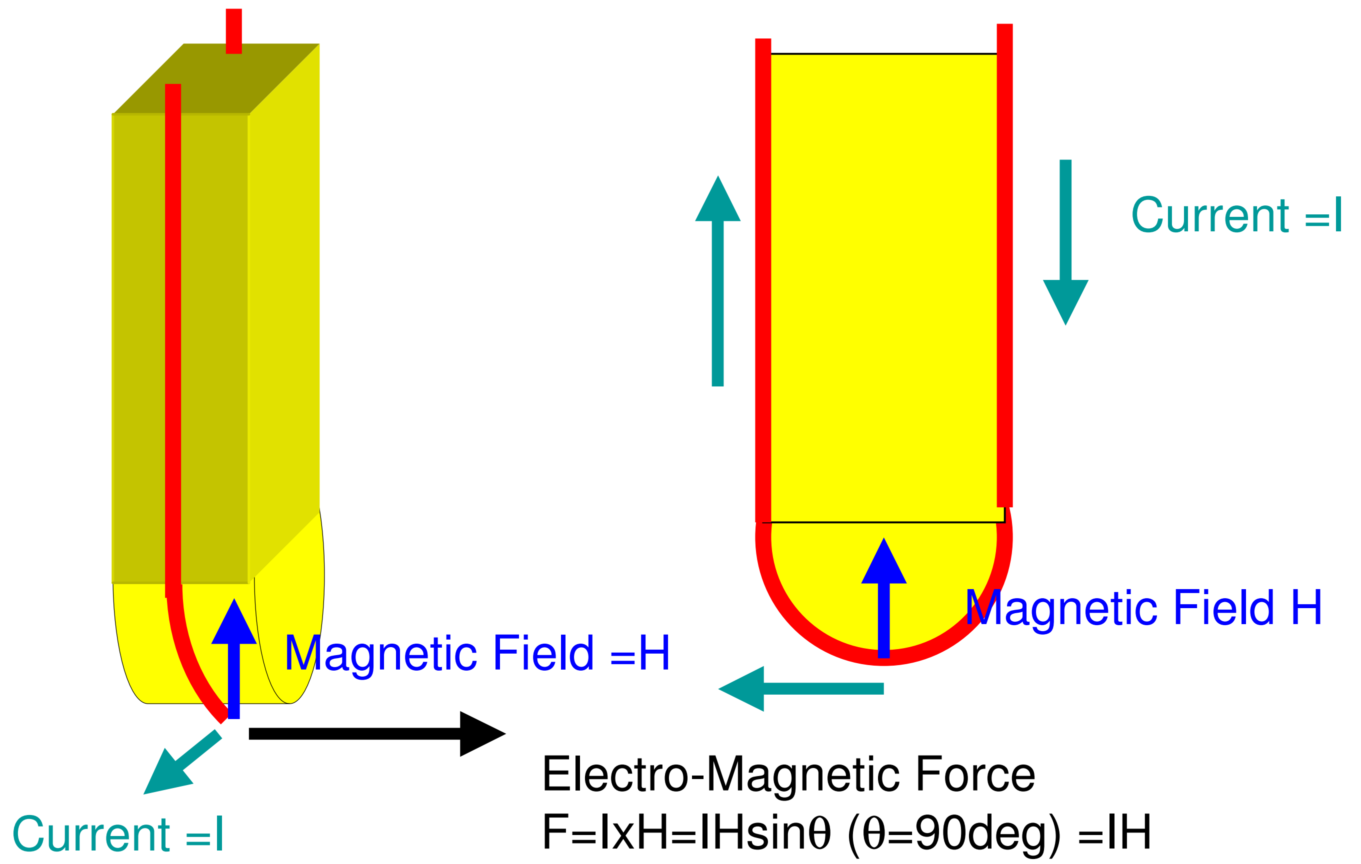

Electro-Magnetic force at the bottom of the experimental system for observation of wire motion

Principle of Measurement 1

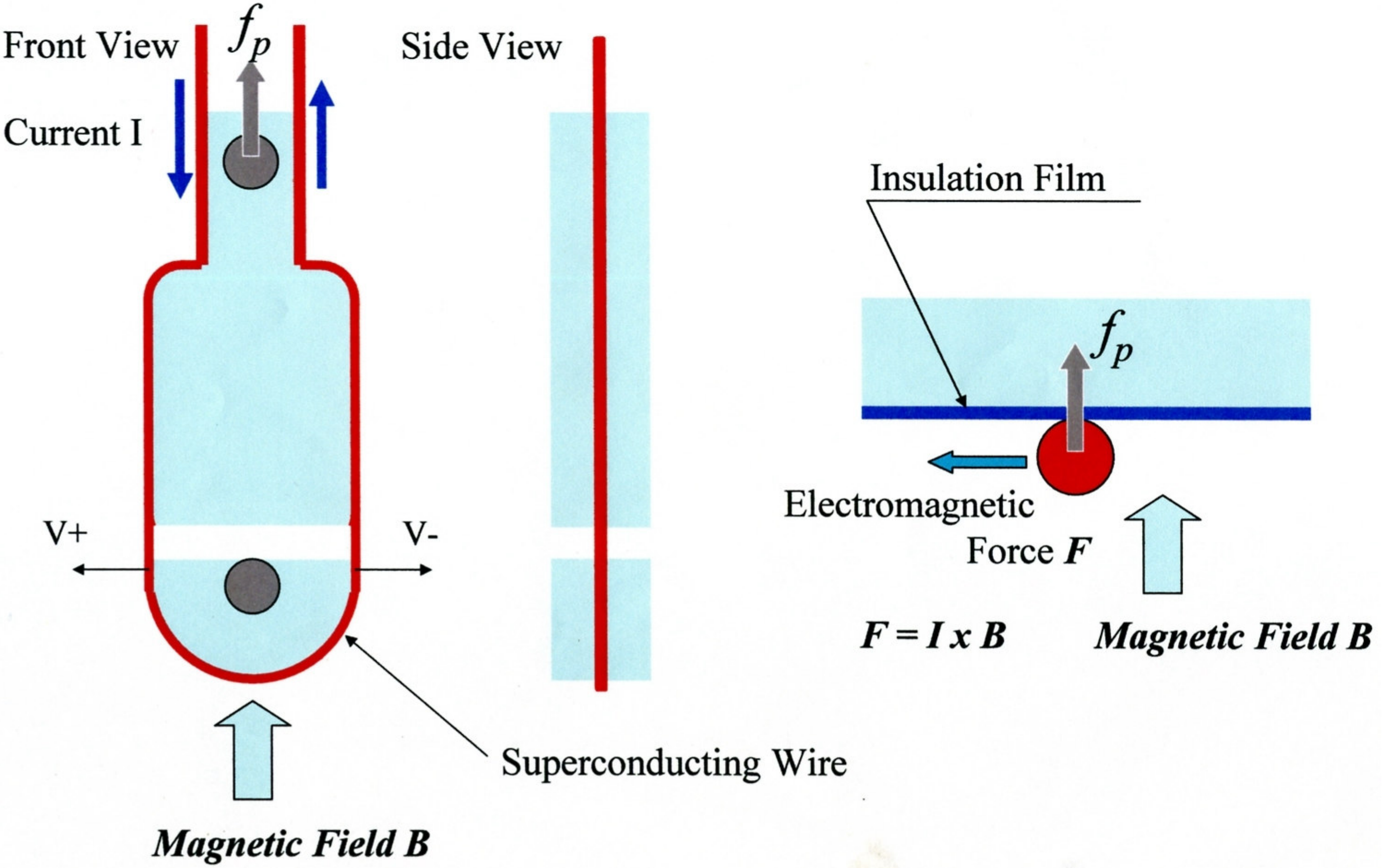

Principle of Measurement 2

Backup field B will be kept constant!

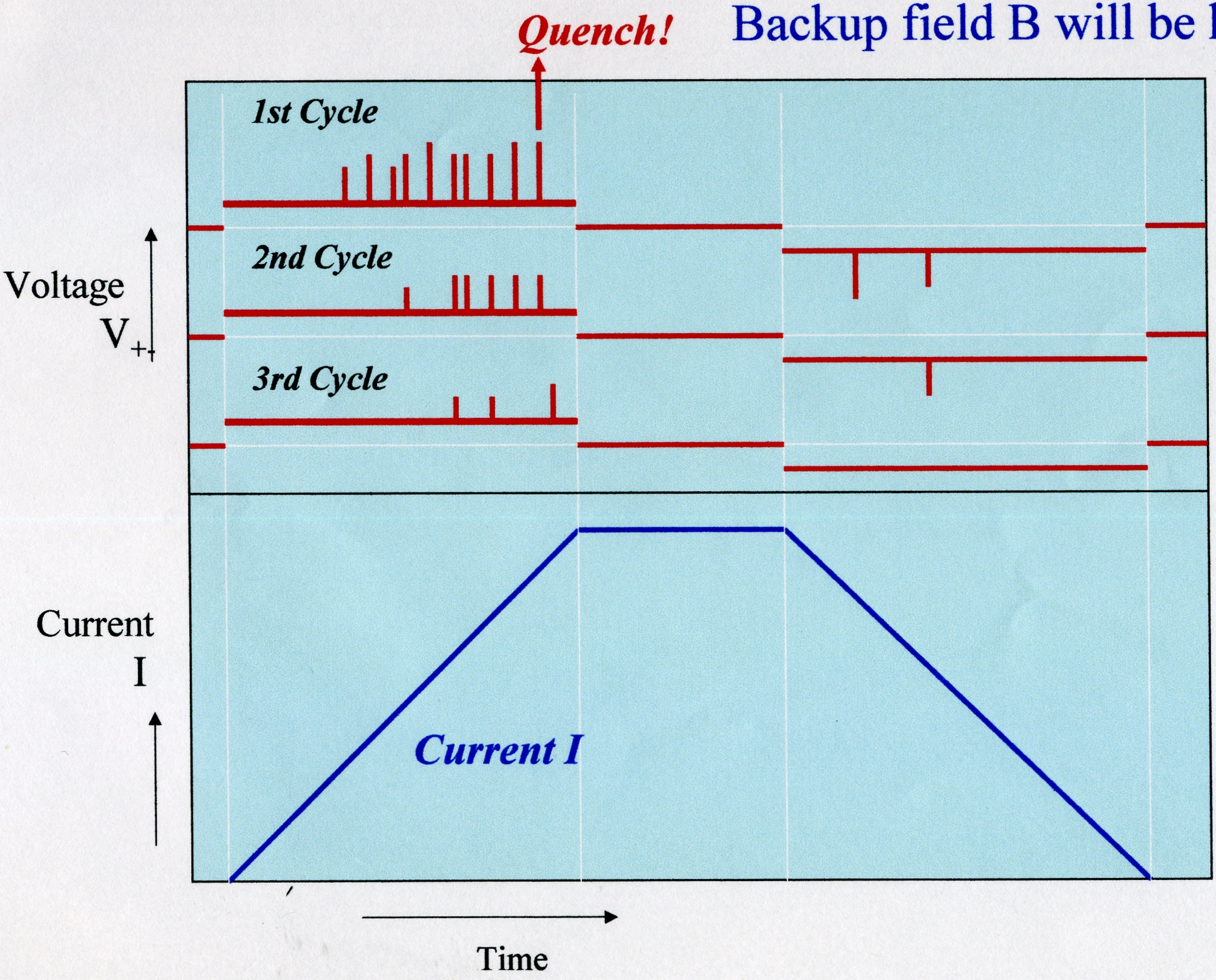

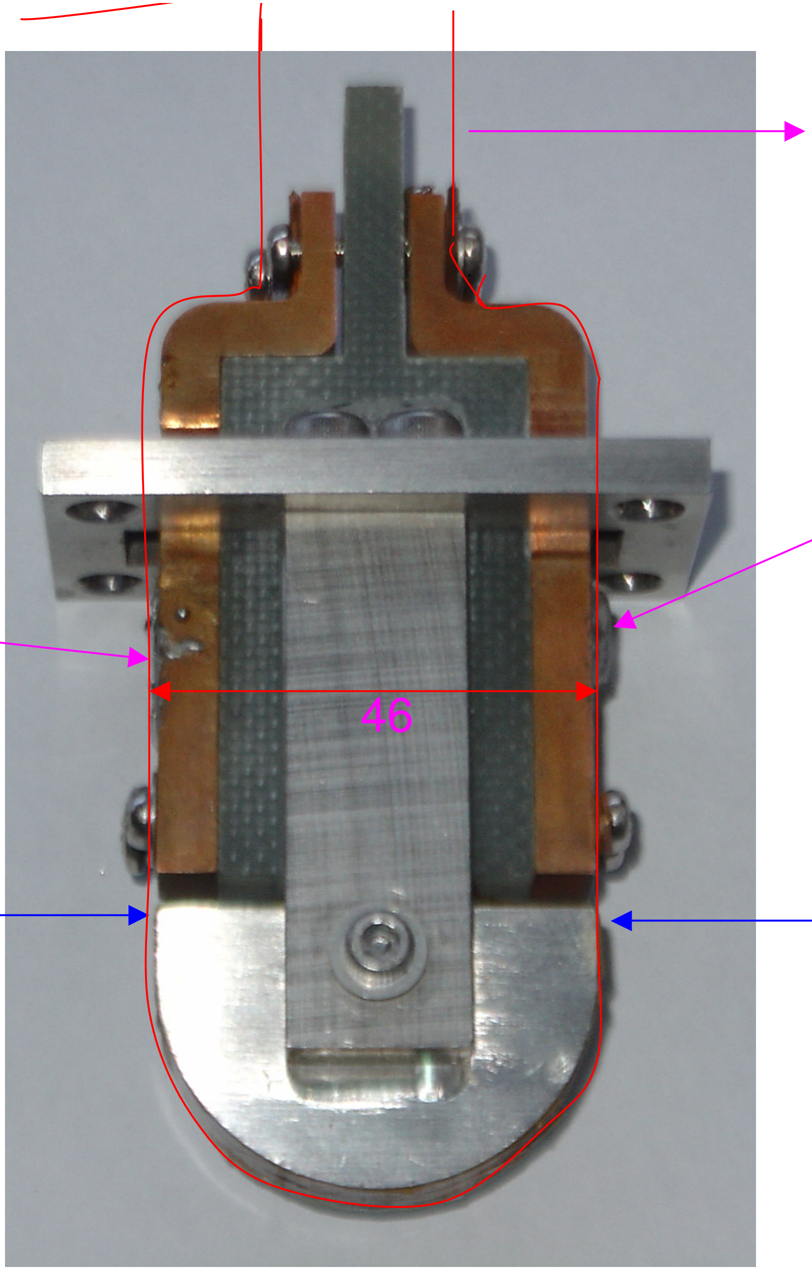

Sample holder

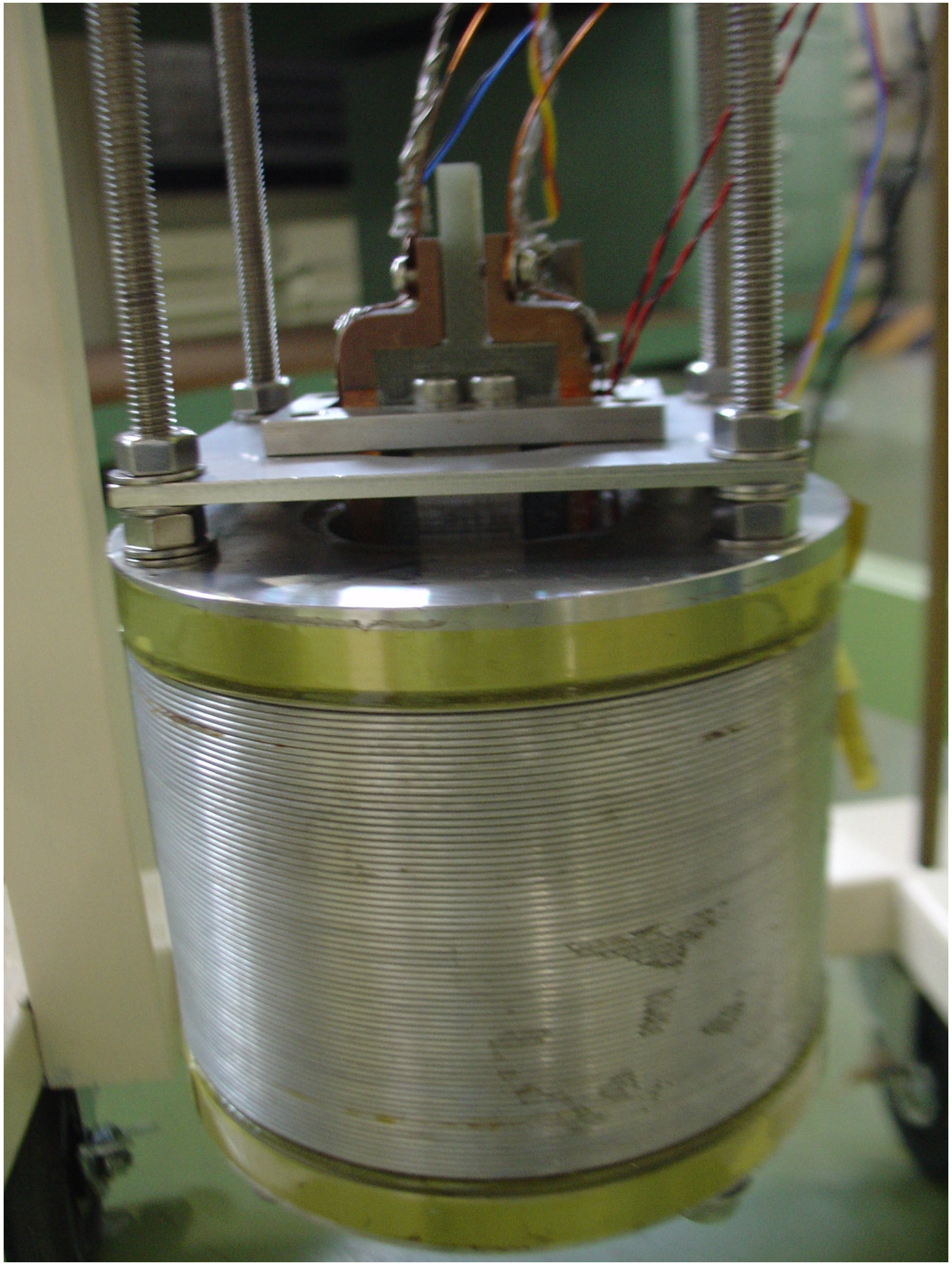

Sc wire characteristics of specimen wire

• Wire diameter	0.7 mm
• Filament diameter	6 µm
• No. of Filaments	10,000
• Pitch length	30 mm
• Cu/NbTi	1:1.8
• Ic	383 A @ 4T
	100 A @ 8.57 T

Characteristics of high strength polyethylene fiber (DYNEEMA®) reinforced plastic

- The Dyneema fiber is an ultraoriented polyethylene fiber fabricated by a super drawing method.

- The Dyneema fiber has expansion property longitudinal to the fiber direction during cooling down from room temperature to coil-operating temperature.

- Low frictional coefficient and slides smoothly at 4.2 K.

- Heat conductivity is as high as that of steel.

Source: http://www.toyobo.co.jp/e/seihin/dn/dyneema/index.htm

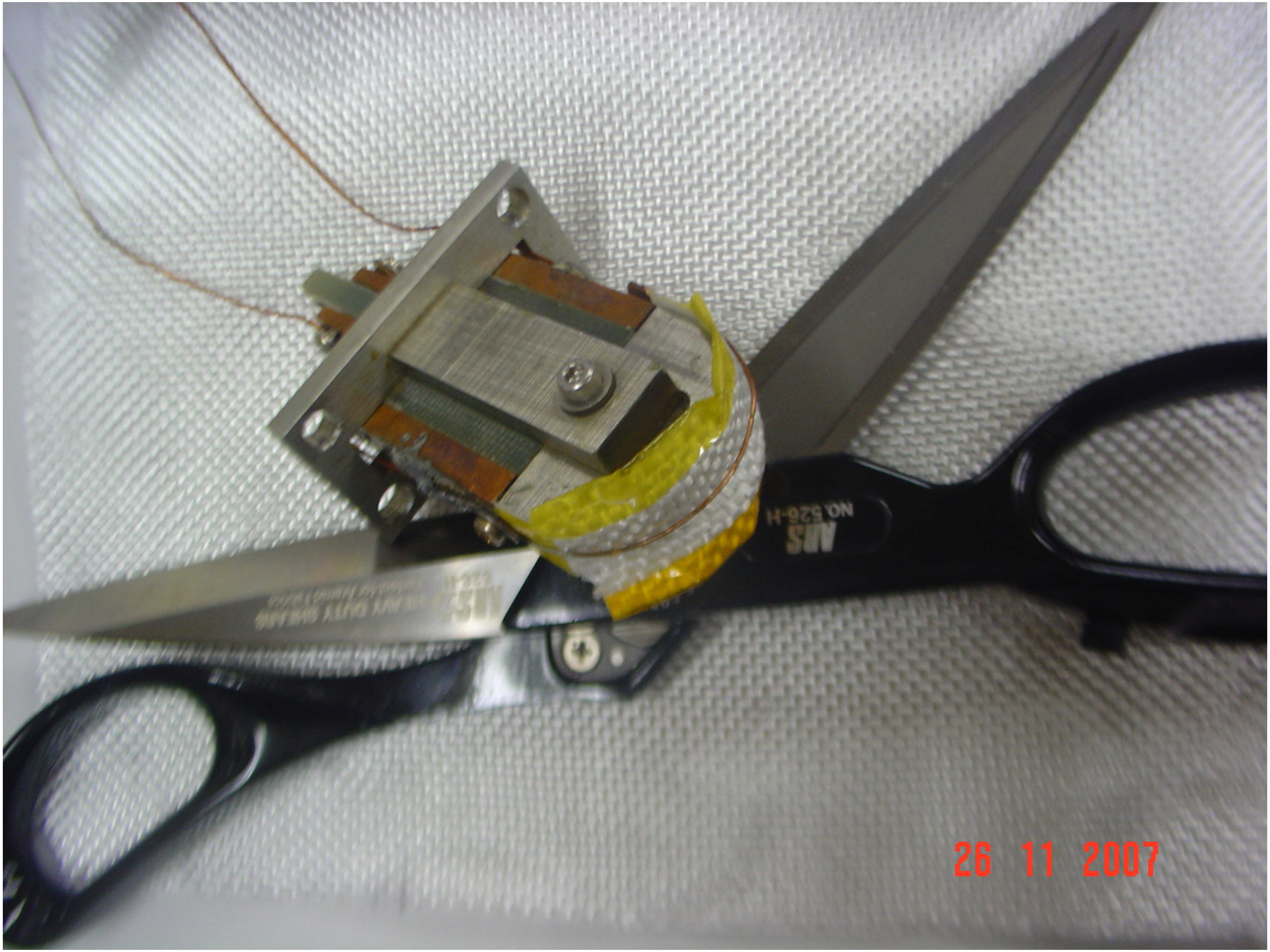
26 11 2007

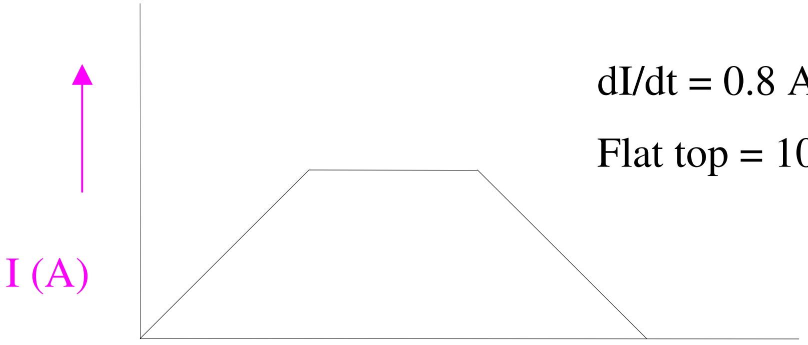

Backup field = 5 T

Load = 0.8 Kg (Polyimide film)

= 0.2 Kg (Dyneema)

Current waveform applied to Sc wire

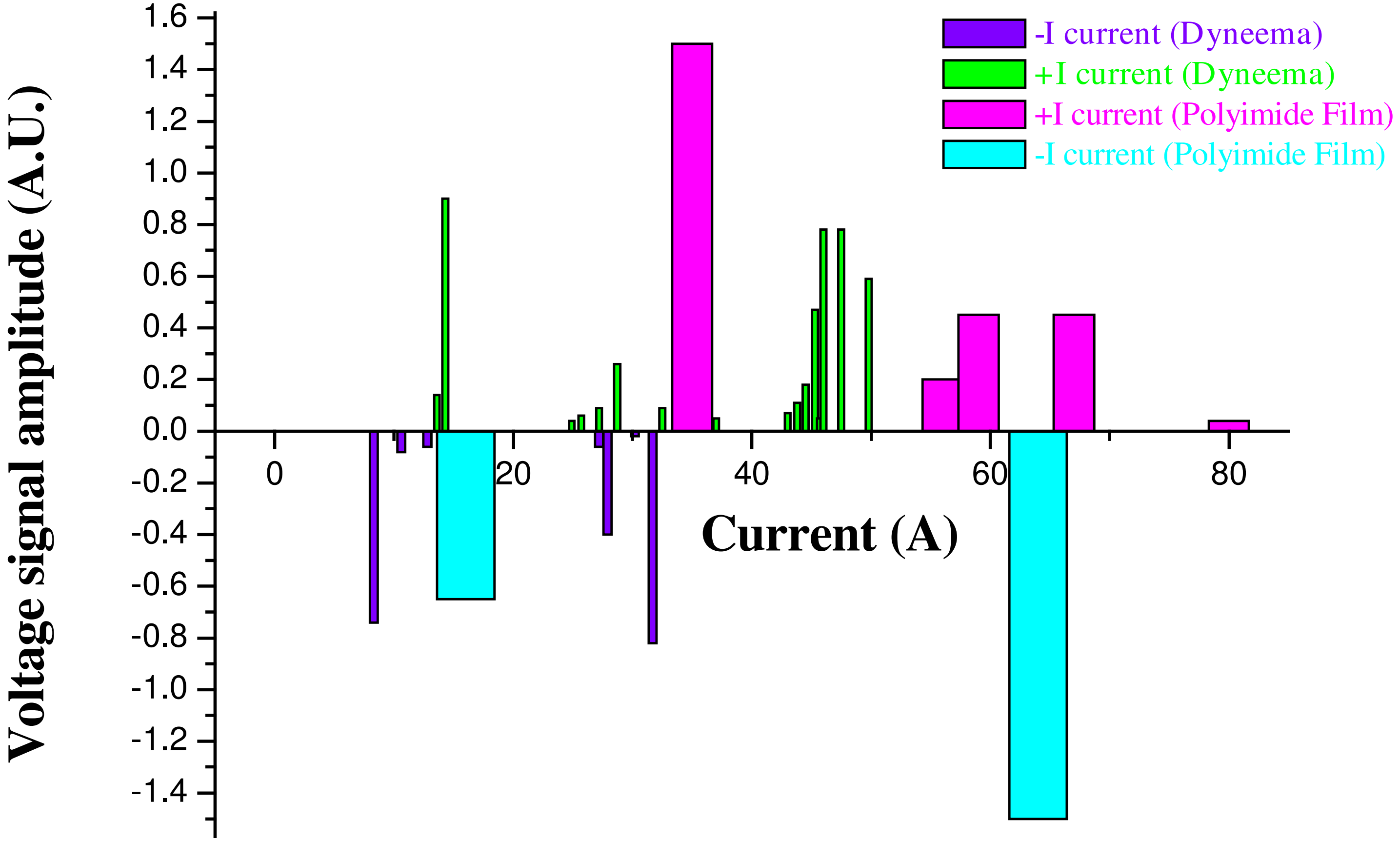

THANKS FOR YOUR KIND ATTENTION

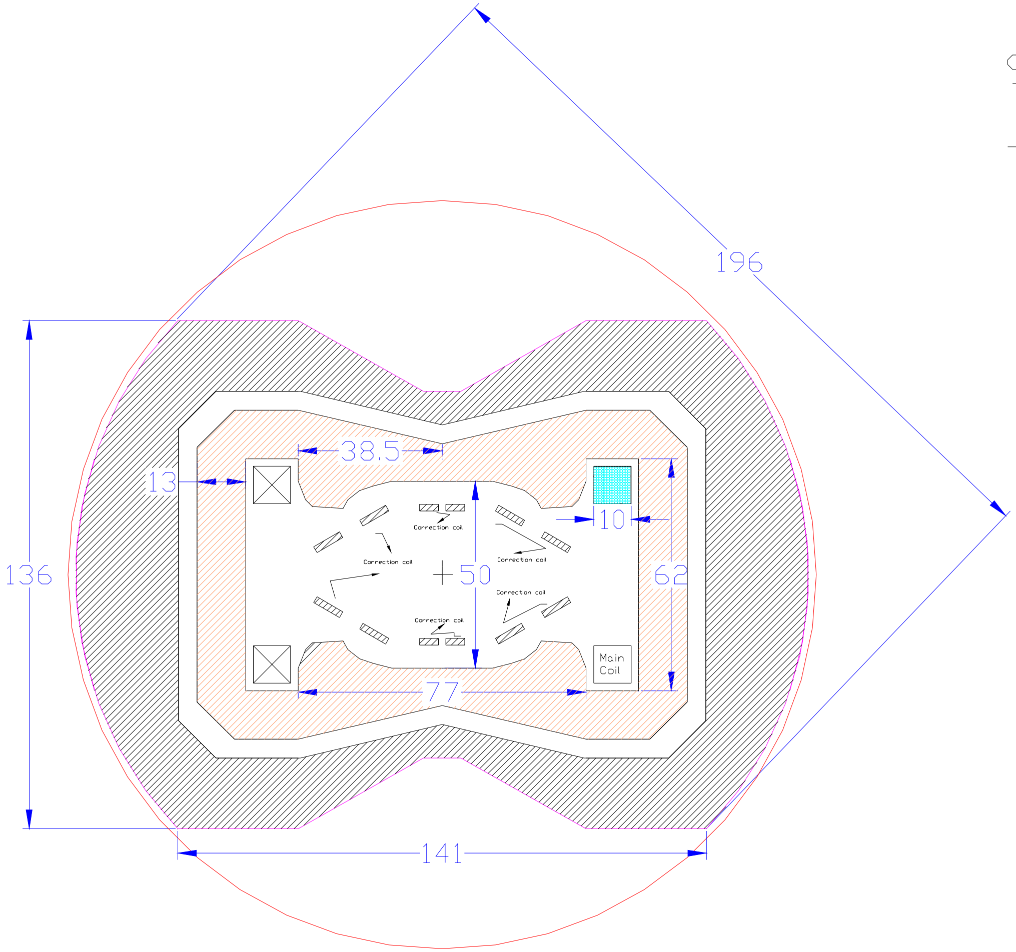

Cross-section of magnet

Iron weight @ 4.2 K 2.68 Kg

Iron weight @ 77 K 4.73 Kg

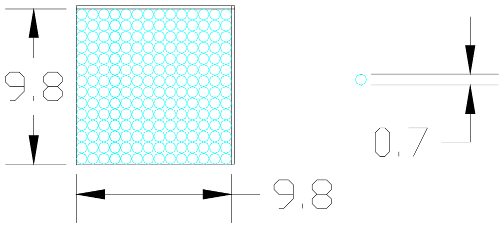

Turns (HxV)

(14x14)

Main Coil

Inductance = 0.13 H

Turns (HxV)

(20x7)

Turns (HxV)

(32x7)

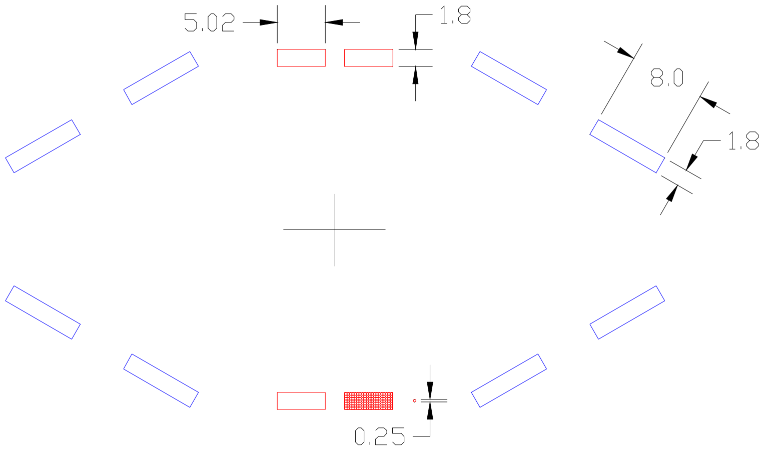

Self-Correction Coil

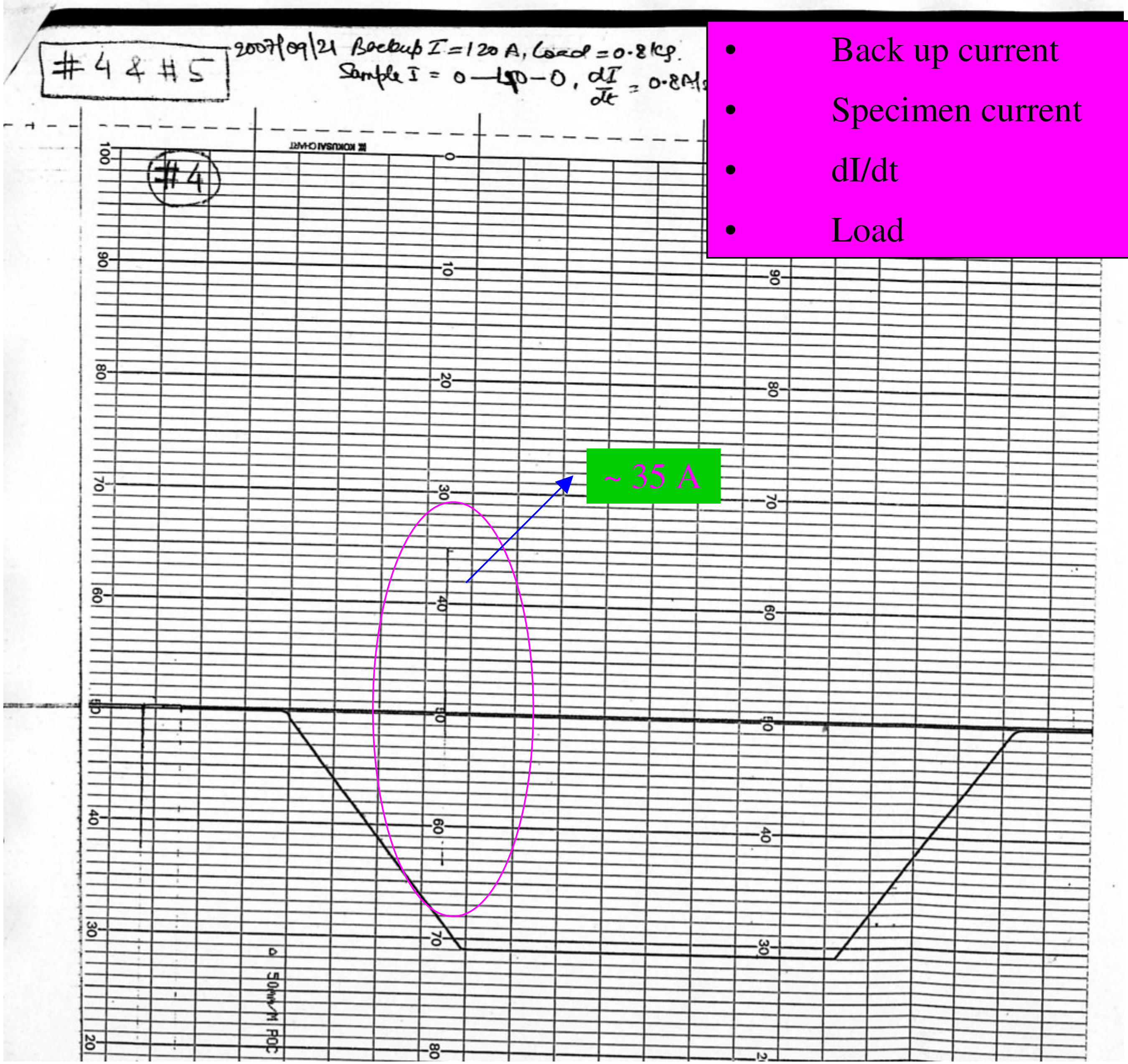

- Back up current 120 A (Fix)
- Specimen current 0 → 40 →0
- dI/dt 0.8 A/s
- Load 0.8 Kg

Super drawing method

- Ultra-high molecular weight polyethylene is dissolved in a solvent and then spun through small orifices (spinneret). Successively, the spun solution is solidified by cooling, which fixes a molecular structure which contains a very low entanglement density of molecular chain. This structure gives an extremely high draw ratio and results in extremely high strength. The gel-like appearance of the solidified fiber is the origin of the name of this technology. The highly drawn fiber contains an almost 100% crystalline structure with perfectly arranged molecules, which promotes its extremely high strength, modulus, and other excellent properties.

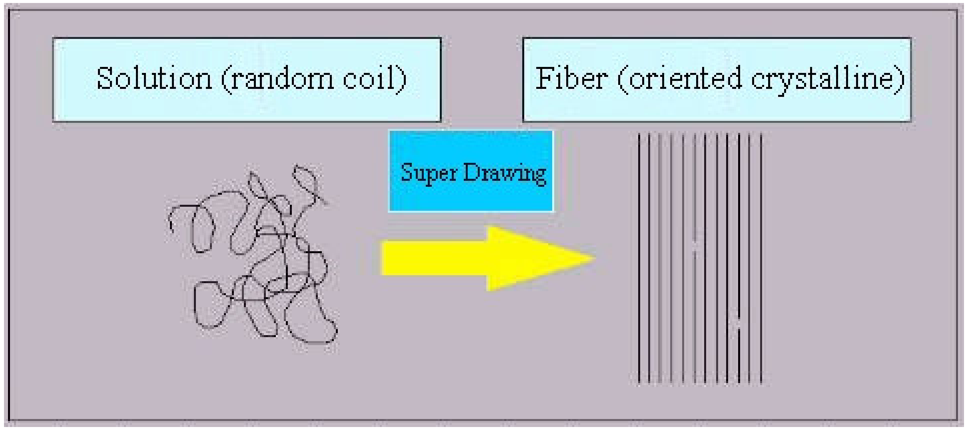

Source: http://www.toyobo.co.jp/e/seihin/dn/dyneema/koutei/index.htm

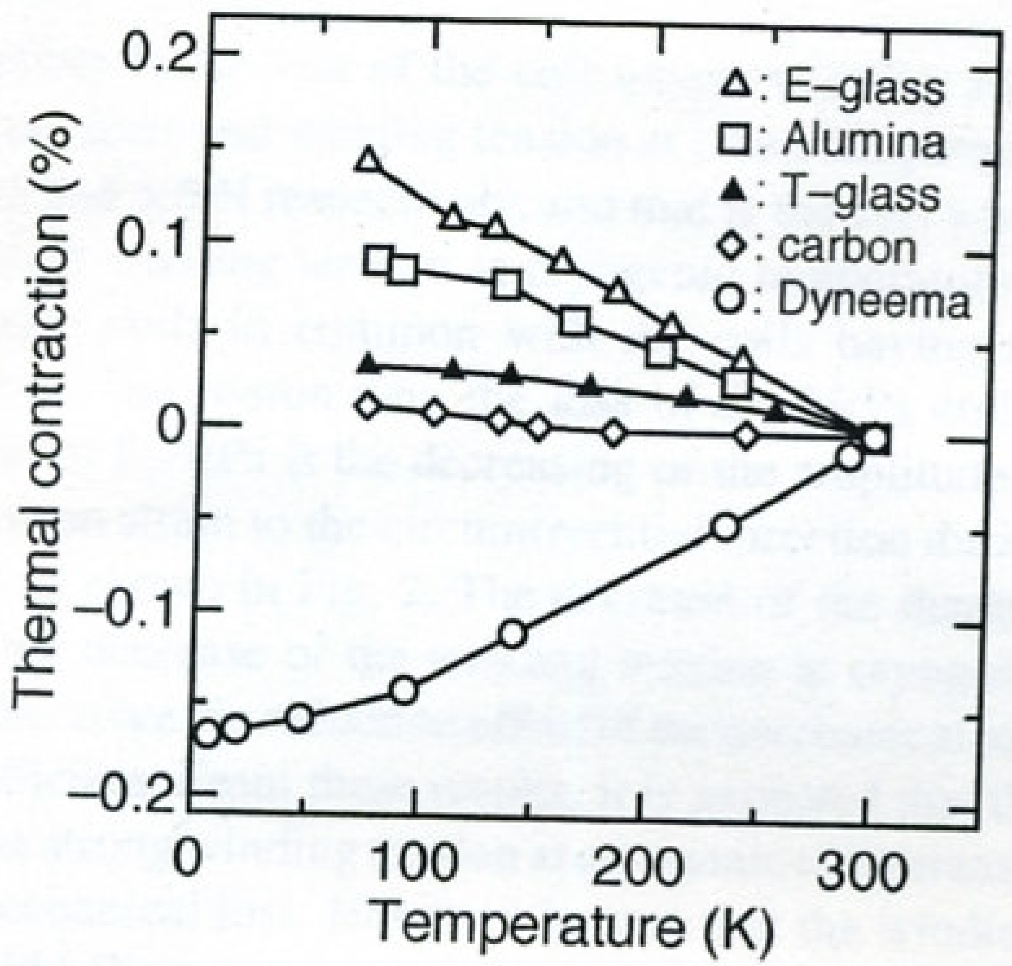

Thermal contraction strains of plastics reinforced by various fibers

Ref.: Naoki Sekine et al., IEEE Trans. On Appl. Supercond., Vol. 14, No. 2, June 2004

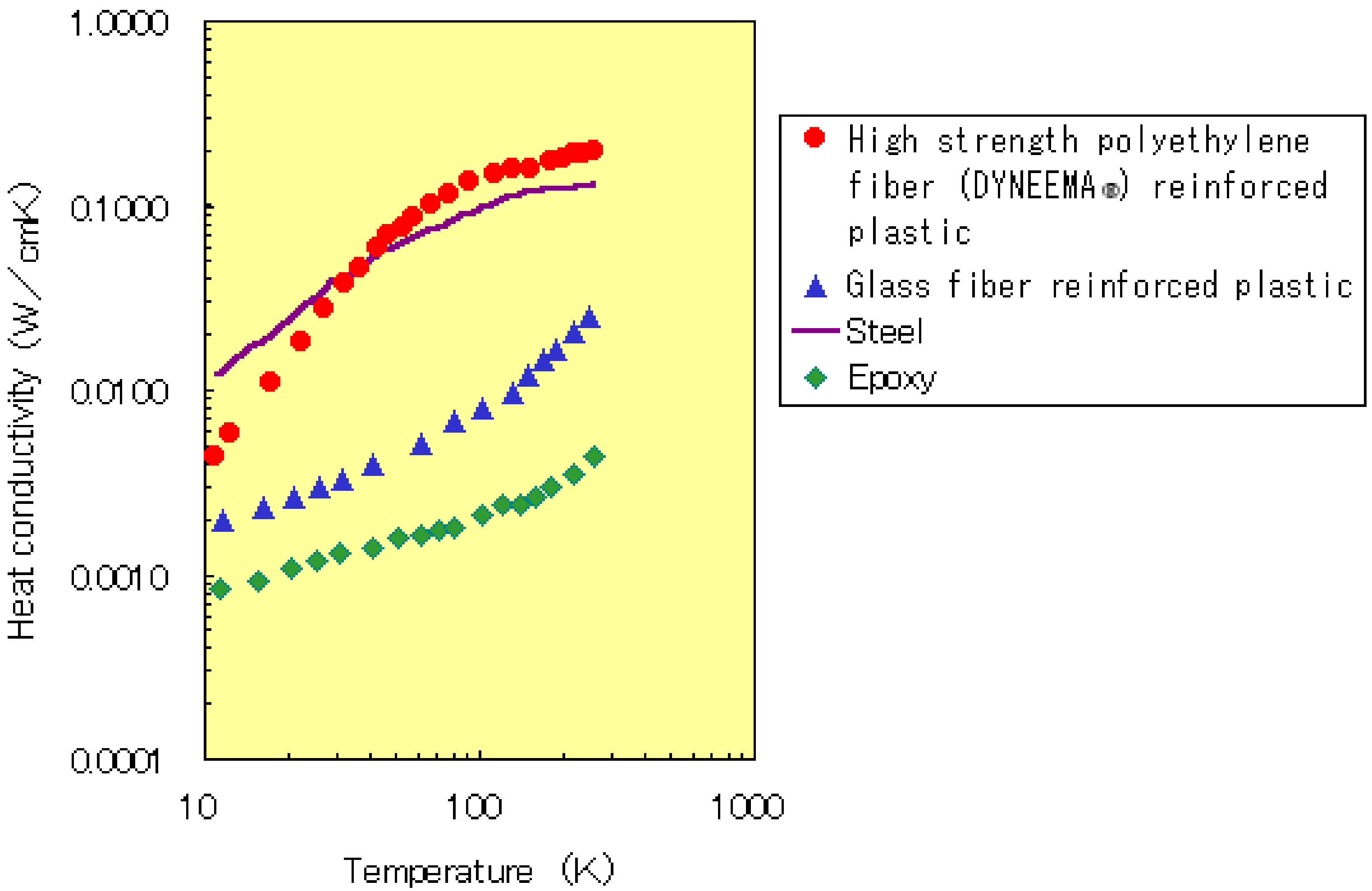

High heat conductivity

Source: http://www.toyobo.co.jp/e/seihin/dn/dyneema/index.htm

FAIR @ GSI, Darmstadt, Germany

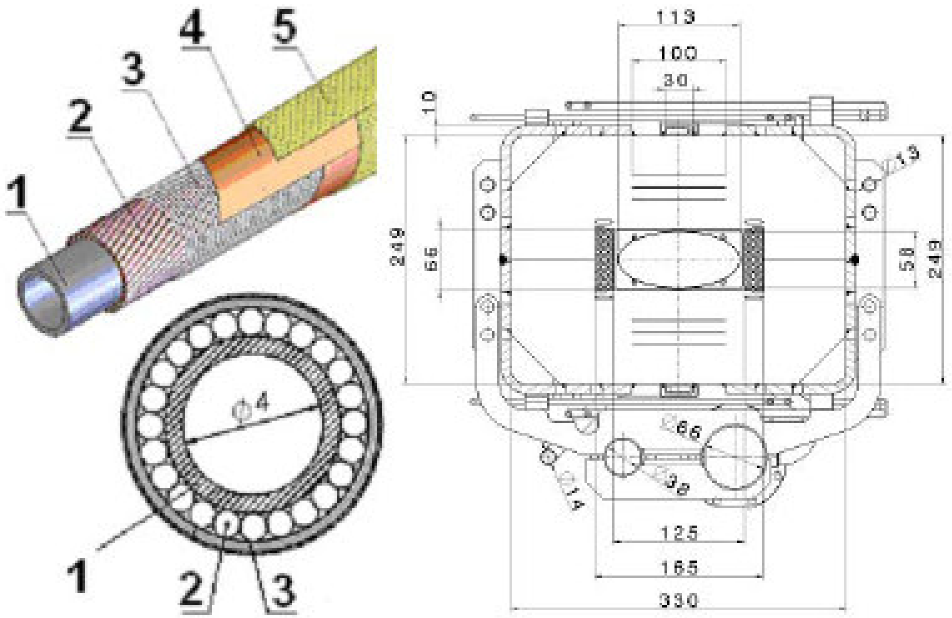

Figure 3: SIS100 dipole with Nuclotron type cable (1- cooling tube, 2 - Superconducting wire, 3 - Nichrome wire, 4 - Kapton tape, 5 – adhesive Kapton tape).

Figure 4: Comparison of resistive and superferric magnets.

Field	1.9 T
Ramp rate	4 T/s
Usable aperture	115x60mm
Magnetic length	2.756 m
No. of magnet	108
Stored energy	4.8 MJ
Cycle length	1.8 s
Lamination	0.5 mm
Total mass	1600 Kg

Strand Diameter	~ 4 μm
No. of strands	31
Cooling tube	Cu-Ni
Current	6.5 kA

Conductor development is in R&D phase

Ref.: G. Moritz, Proc. PAC07

•Superferric quadrupole triplet at RIKEN.

KUSAKA *et al.*: PROTOTYPE OF SUPERFERRIC QUADRUPOLE MAGNETS FOI

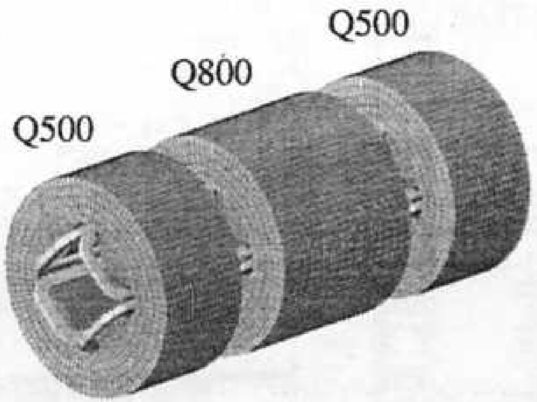

Fig. 1. Schematic view of the prototype quadrupole triplet.

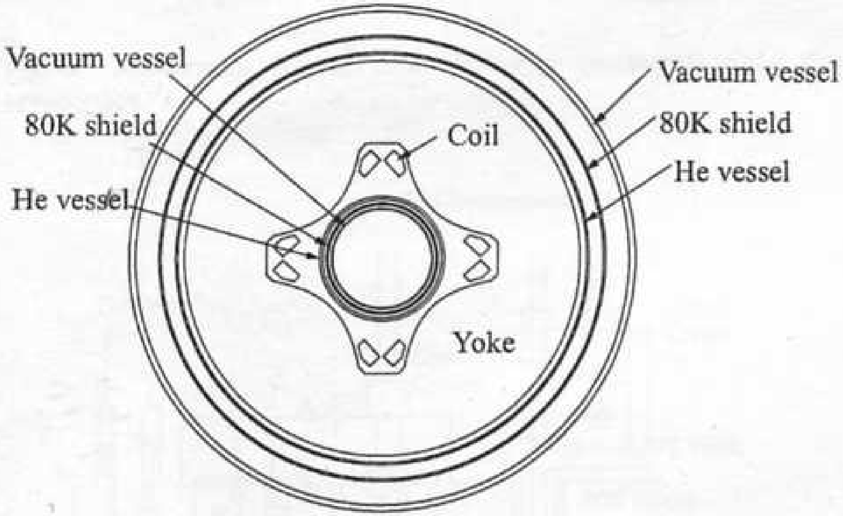

Fig. 2. Cross-sectional view of the prototype quadrupole.

Gradient	14.1 T/m
Pole radius	170 mm
Worm bore radius	140 mm
Magnetic length	0.54/0.84 m
Stored energy	0.13 MJ
Outer radius of yoke	480 mm

Strand Diameter	~ 75 μm
Insulated diameter	1.15 mm
Cu/super ratio	6.6
RRR of Cu	100

Ref.: Kusaka et al. IEEE Trans. On Appl. Supercond., Vol. 14, No. 2, June 2004

Superferric Dipole for A1900 Fragment separator

National Superconducting Cyclotron Lab (NSCL)
at Michigan State University, USA.

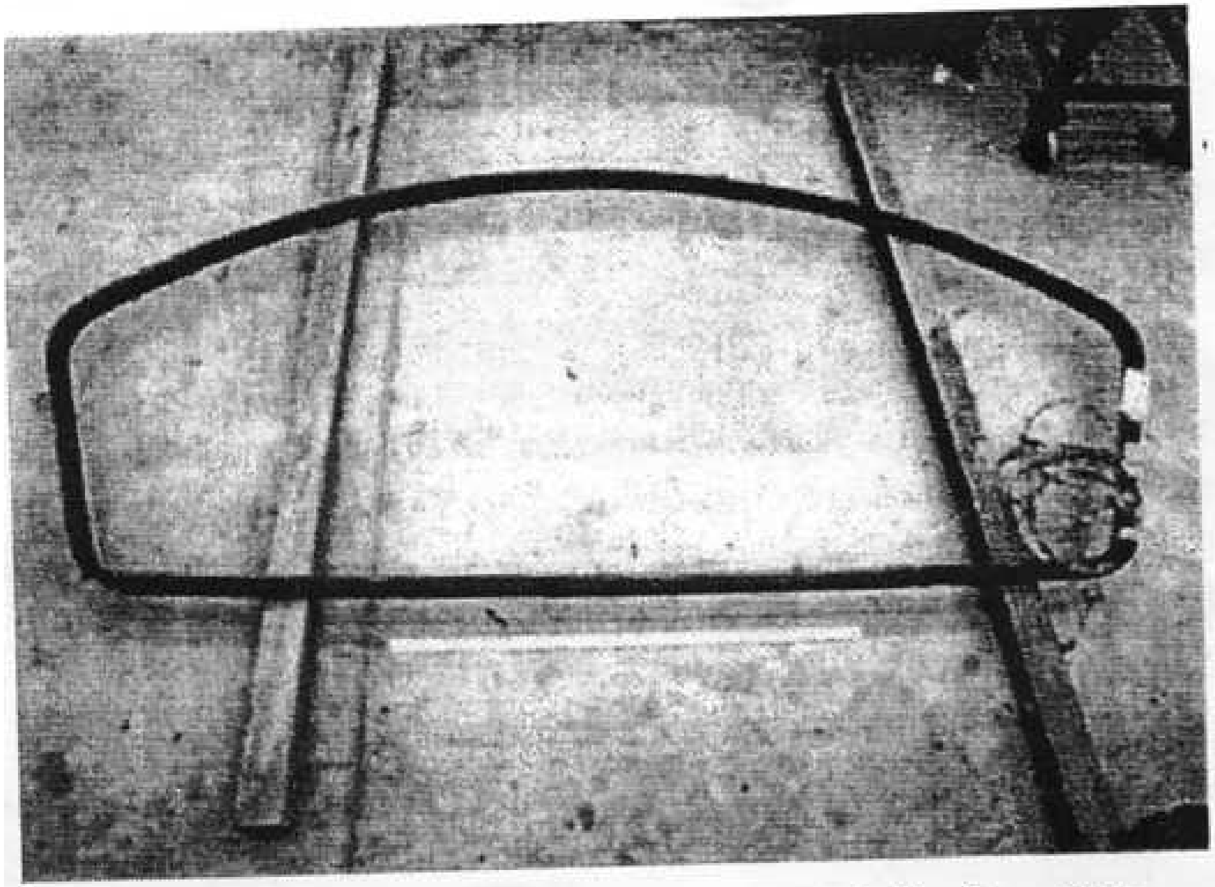

Fig. 2. Complete dipole coil after removal from the winding form. Note meter stick in foreground.

Superferric Dipoles (4 Nos., 45° bend, B=2T),
Superferric Quadrupole Triplets (8 Nos.)

Field	2 T
Pole gap	90 mm
Bend angle	45°
No. of turns	599
Current	171 A
Stored energy	0.5 MJ
Iron mass	50000 Kg
No. of dipole	4
No. of quadrupole	8

Conductor size	0.898 mm x 1.898 mm
Critical current at 2T	~ 500 A

Ref.: Zeller et al. IEEE Trans. On Appl. Supercond., Vol. 11, No. 1, March 2001

Superferric Quadrupole @ 10 Hz

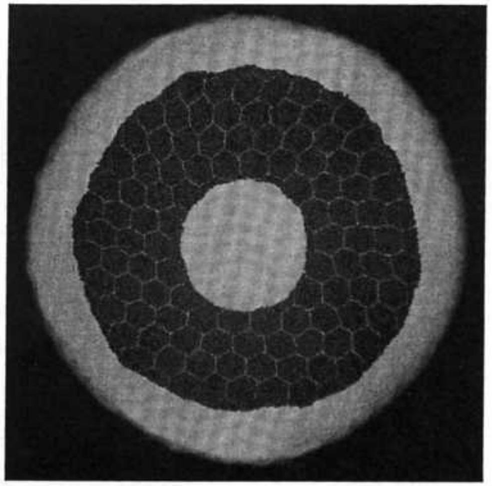

Fig. 2. Microphotograph of the new wire internal structure.

Dynamic heat releases at 32 T/m, 10 Hz	
Coil	65.7 W
Yoke at 80 K	178 W

Gradient	32 T/m
Pole gap	90 mm
No. of turns	4x2
Current	13.1 kA
Stored energy	6.0 kJ
Iron mass	200 Kg

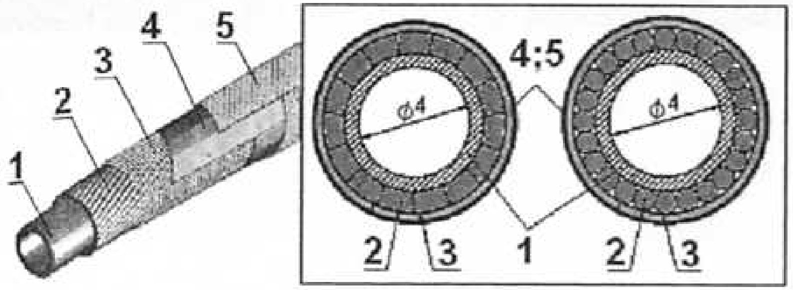

Fig. 6. Hollow cables: left—standard Nuclotron, made with 31 wires of 0.5 mm diameter; inside the frame: left—the KWAT1 cable [4], right -the HCC2 cable consisting of 24 wires 0.73 mm diameter. 1—copper nickel tube with channel for two-phase helium flow, 2—NbTi wire, 3—nichrome wire, 4—Kapton tape, 5—glass-fiber tape.

Characteristics	KWAT1	HCC2
Cu-Ni tube diameter	5 mm	5 mm
Cable outer diameter	7.32 mm	7.32 mm
No. of strands	15	24
Strand cross-section	0.785 mm^2	0.419 mm^2
Matrix/SC ratio	1.8	1.92
Filament diameter	5.8 μm	4.2 μm
Filament twist pitch	11 mm	7 mm
Operating current	13.4 kA @ 2 T, 4.6 K	13.1 kA @ 2.4 T, 4.4 K

Ref.: Khodzhibagiyan et al. IEEE Trans. On Appl. Supercond., Vol. 17, No. 2, June 2007

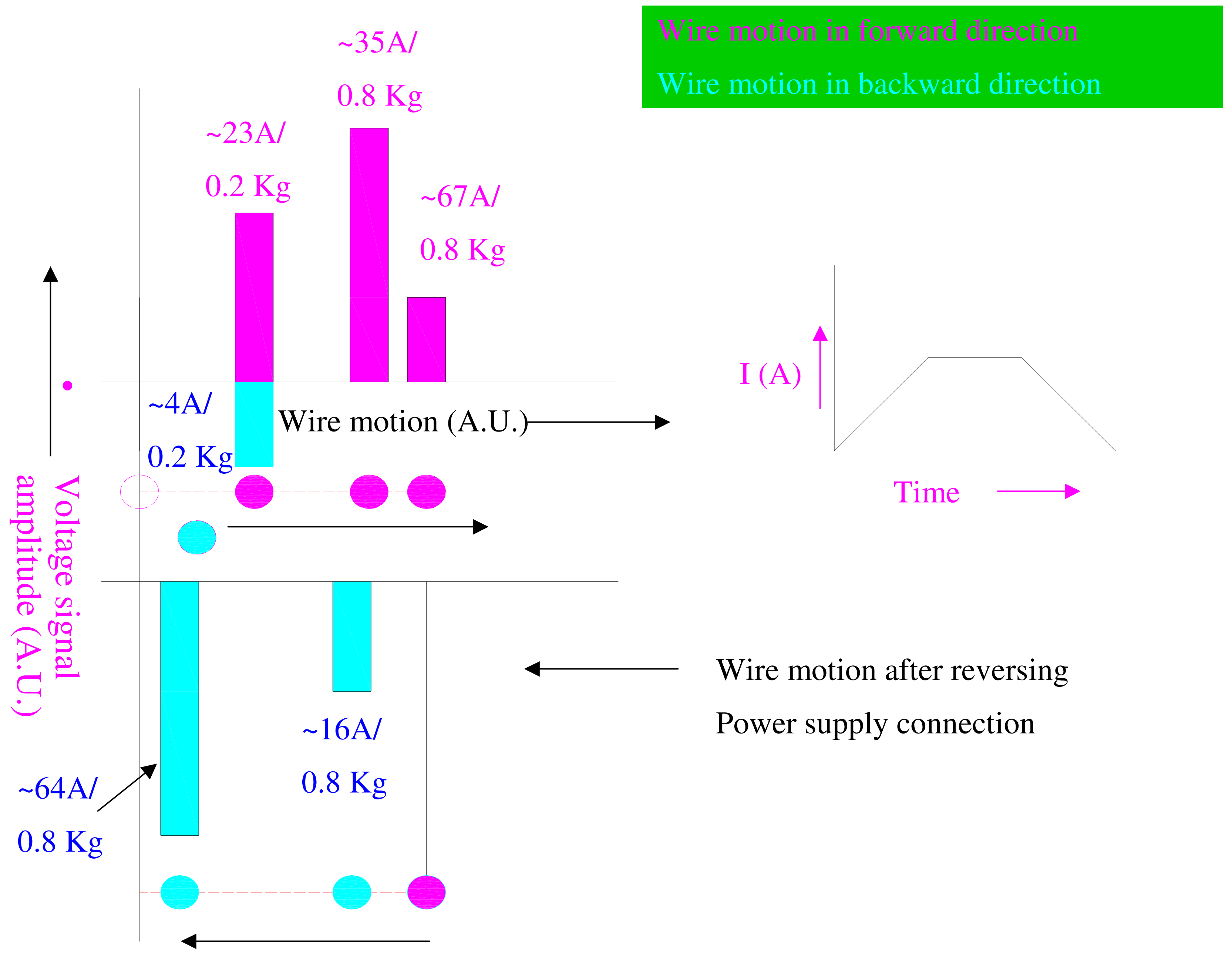

Wire motion in forward direction
Wire motion in backward direction
~35A/
0.8 Kg
~23A/
0.2 Kg
~67A/
0.8 Kg
~4A/
0.2 Kg
Wire motion (A.U.)
Voltage signal
amplitude (A.U.)
I (A)
Time
~16A/
0.8 Kg
~64A/
0.8 Kg
Wire motion after reversing
Power supply connection

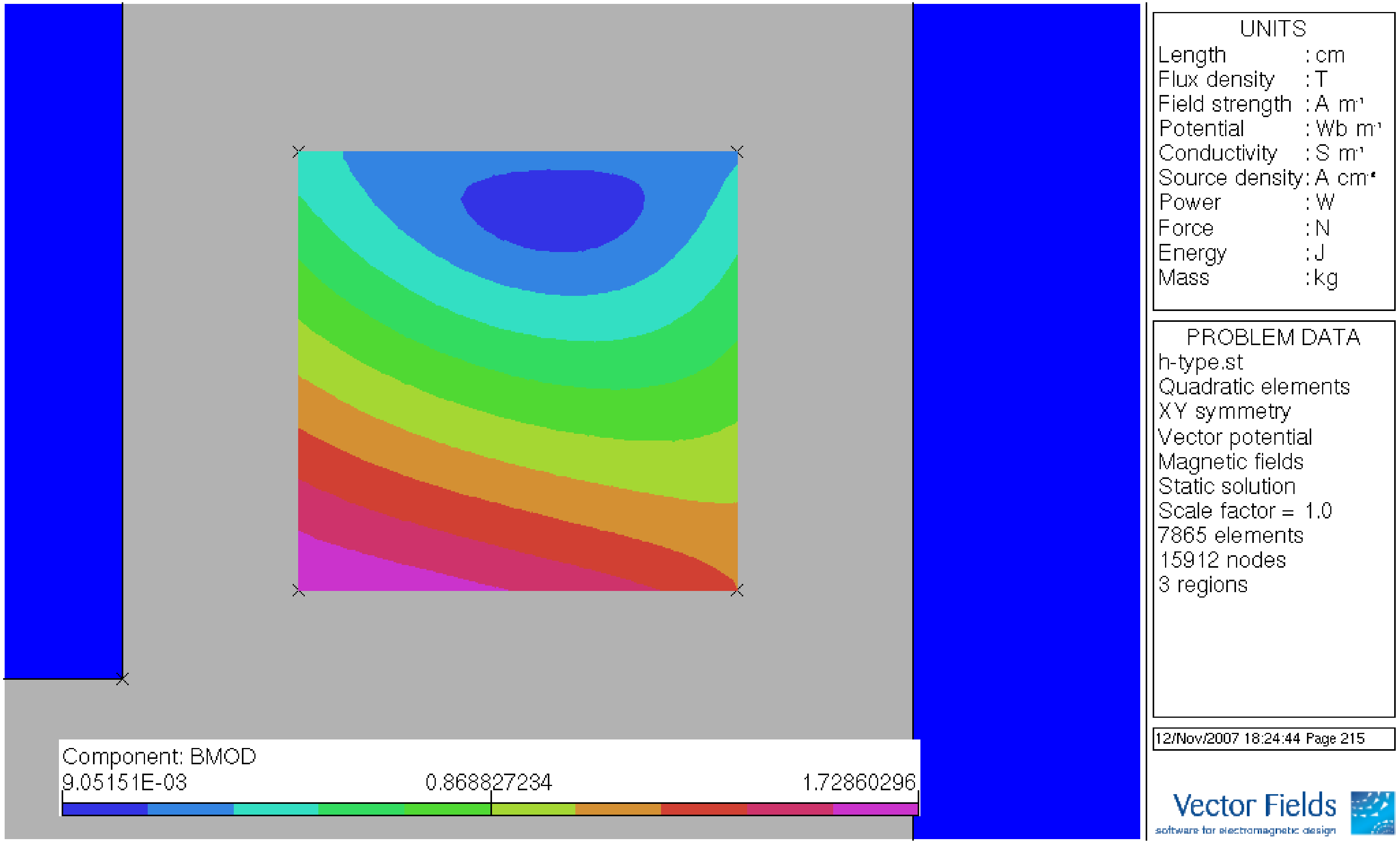

Field inside Main Coil

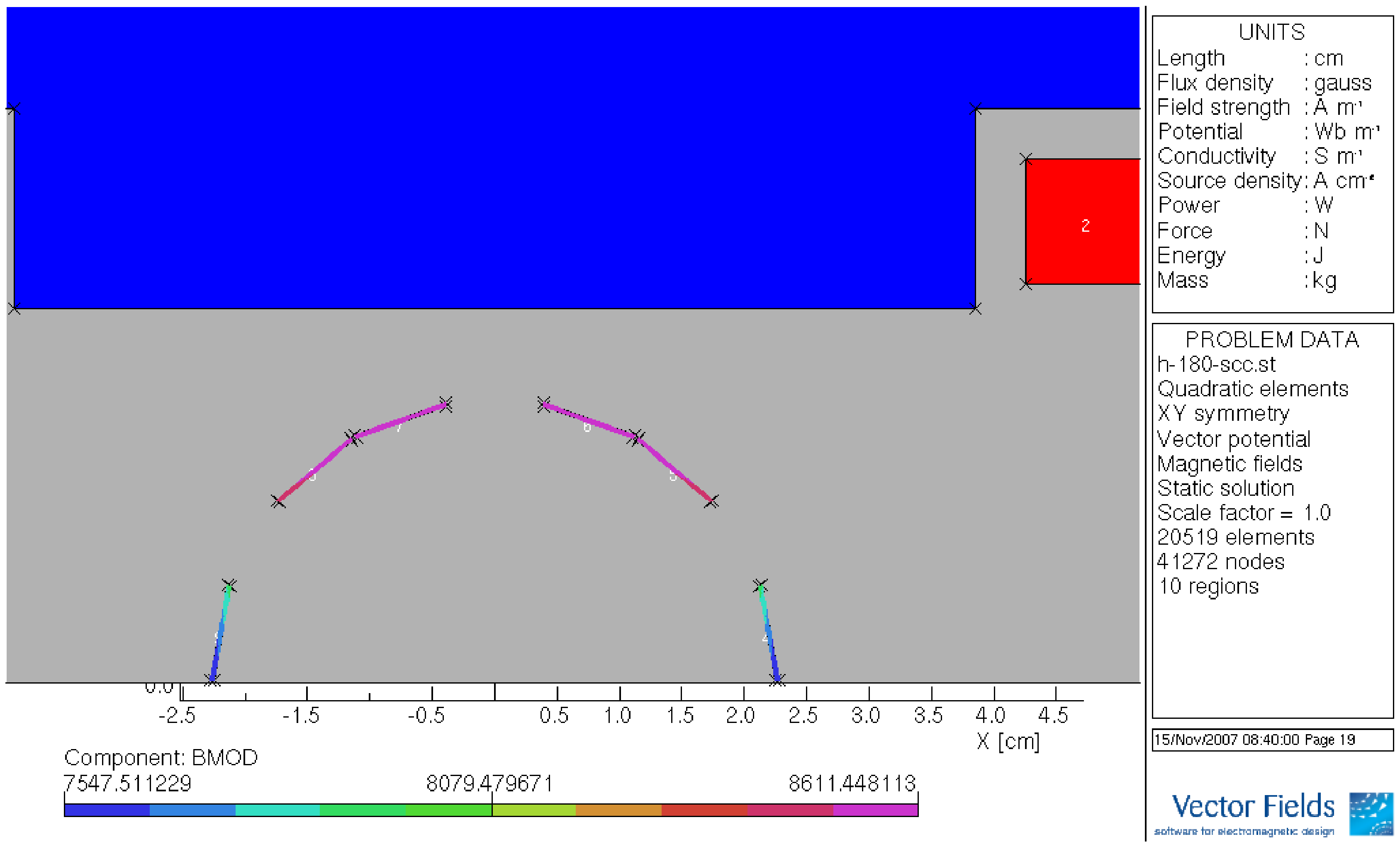

Field inside SCC